Thin Solid Films 580 (2015) 21–28

Contents lists available at ScienceDirect

Thin Solid Films

journal homepage: www.elsevier.com/locate/tsf

Roll-offset printed transparent conducting electrode for organic solar cells

Inyoung Kim *, Sun-Woo Kwak, Yeonkyeong Ju, Gun-Young Park, Taik-Min Lee, Yunseok Jang, Young-Man Choi, Dongwoo Kang

Department of Printed Electronics, Korea Institute of Machinery and Materials (KIMM), 156 Gajeongbuk-ro, Daejeon 305-343, Republic of Korea

ARTICLE INFO

Article history:
Received 12 August 2014
Received in revised form 27 February 2015
Accepted 27 February 2015
Available online 6 March 2015

Keywords:
Silver
Nanoparticles
Transparent conducting electrodes
Organic solar cells
Printed electronics

ABSTRACT

Transparent conducting electrodes (TCEs) were developed through the roll-offset printing of Ag grid mesh patterns for the application of all-solution processed organic solar cells (OSCs). Due to the remarkable printability of roll-offset printing, the printed TCEs did not show the step coverage problem of subsequent thin layers, which was a chronic problem in other printing techniques. The control of ink cohesion was verified as a critical factor for the high printing quality, which was optimized by adding a polyurethane diol of 2 wt.%. The tensile strength of optimized Ag ink was 322 mN, which led to the clear patterning of Ag nanoparticles. The printed TCEs with different mesh densities of the Ag grid were designed to have a similar property of indium tin oxide (ITO). The measured sheet resistance was 13 Ω/□, and optical transmittance was 86%, including the glass substrate, which was found to be independent of wavelength in the visible spectrum, in contrast with the optical transmittance of ITO. To evaluate the TCE performance as bottom electrodes, all-solution processed OSCs were fabricated on top of the TCEs. The power conversion efficiency (PCE) of the OSCs increased with the increments of the mesh density due to the distinctive increase of the short circuit current density (J_{sc}), notwithstanding the similar transmittance and sheet resistance of the TCEs. In comparison with ITO, a higher PCE of OSCs was obtained because the printed TCEs with a high mesh density were able to facilitate effective current collection, leading to a significant increase of J_{sc}.

1. Introduction

Printing techniques are emerging as a manufacturing method of electronic devices due to their advantages of cost effectiveness and environmental friendliness. Various types of printed electronic devices, such as light emitting devices (LEDs) [1,2], thin film transistors [3,4], solar cells [5,6], batteries [7,8], and sensors [3,9], have been studied using solution based ink materials. Among these applications, organic solar cell (OSC) is regarded as most practicable for large-area printing on flexible substrates due to the solution-based simple manufacturing processes including low-temperature treatment [10]. In recent years, the power conversion efficiency (PCE) of polymer bulk heterojunction OSCs has increased up to 11% with the development of low-band gap polymers [11,12], device structures [13], and the optimization of processing variables, such as the solvent evaporation time [14] and the annealing conditions [15]. On the other hand, the use of indium tin oxide (ITO) as a transparent conducting electrode (TCE) can hinder the progress towards low-cost and large-area flexible devices because ITO still exhibits high cost due to the scarcity of indium. Furthermore, the band structure of ITO is not optimized for solar cell application, which hinders efficient photocurrent generation [16,17]. Thus, a number of studies have addressed the development of alternative TCEs using the large area printing of metal nanoparticles or nanowires [5,6,18].

Recently, roll-offset printing has attracted much attention due to its outstanding printability [19]. While gravure, offset, flexo, or inkjet printing techniques have revealed the limitations on the control of a clear line shape, thickness and line width [4,6,19,20], roll-offset printing realized higher printing resolution of 1–3 μm line width with a smooth thin film surface of ~3.5 Å roughness [19]. In addition, the thickness of roll-offset printed thin film was controllable from several hundred nanometers to micrometers by changing the nanoparticle concentration of the colloid as well as the coating conditions. The roll-offset printing involves several complicated processes: 1) coating, 2) off, 3) patterning, and 4) set, as shown in Fig. 1. In the coating process of Fig. 1(a), ink is coated onto a PDMS bottom blanket with a uniform thickness. The coated ink is entirely transferred from the bottom blanket to the roll blanket in the second process of Fig. 1(b). The transferred ink on the PDMS roll blanket is patterned by cliché in the third process of Fig. 1(c). Then, the patterned ink on the PDMS roll blanket is completely transferred to the substrate. During these roll-offset printing

* Corresponding author.
E-mail address: ikim@kimm.re.kr (I. Kim).

http://dx.doi.org/10.1016/j.tsf.2015.02.075

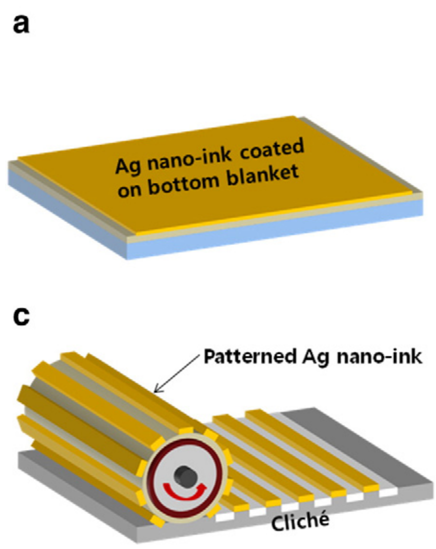

Fig. 1. A schematic illustration of the roll offset printing process composed of four processes: (a) coating, (b) off, (c) patterning, and (d) set.

processes, the coated ink experiences only complete ink transfer without ink separation. Thus, both the thickness and the surface roughness of the roll-offset printed patterns can be controlled by the coating process, and the line shape can be affected by the third and fourth processes.

This study aims to develop highly transparent TCEs via the roll-offset printing of Ag nano-ink for the application of OSCs. ITO-free all printed OSCs have the potential to become competitive with commercial solar cells, even at much lower efficiencies [21]. The fine patterning and pattern shape control of a nanoparticle film via printing processes is critical to the device application of nanoparticle colloids. However, there is a lack of research on the ink properties related to the printing quality [22,23]. In this study, we focused on the following discussion points: 1) the thin film patterning of Ag nanoparticles, 2) the electrical and optical properties of printed Ag films or mesh grids, and 3) OSC performances depending on the design of printed TCE. These discussions will be helpful to understand the relationship between the rheological property of nanoparticle colloids and printing quality as well as the potential of all-printed energy conversion devices.

2. Experimental details

2.1. Synthesis and formulation of Ag nano-ink

In this study, Ag nanoparticles were synthesized using a widely used polyol process [24–26]. $AgNO_3$ (99+, Aldrich) and polyvinyl pyrrolidone (PVP; Mw ≈ 50,000, Aldrich) were separately dissolved in ethylene glycol (99.8%, Aldrich) at room temperature. The PVP solution was heated to 165 °C, and then, the two solutions were mixed by stirring at 300 rpm. The hot solution reduced $AgNO_3$ to elemental silver, which then consistently formed Ag nanoparticles. The reaction was conducted for only three minutes. Synthesized Ag particles that had an average size of approximately 50 nm were washed with a mixture solution of acetone and tetrahydrofuran and then centrifuged at 2500 rpm.

Ag ink was formulated with dried Ag nanoparticles, the concentration of which was controlled at 20–40 wt.% in the main solvent of ethanol (99%, Aldrich) and ethylene glycol monopropyl ether (EGPE, 99%, Aldrich). To control the ink cohesion, a polyurethane diol solution (PUD, Mn ~320, 88% in H_2O, Aldrich) was added at a concentration of 1–3 wt.%, which was also used as a tackifier.

2.2 . Fabrication of transparent conducting film via roll-offset printing

Ag mesh patterns were printed onto 0.7 mm thick soda lime glass substrates with an area of 50 × 50 mm^2 by using a homemade roll-offset printer, which is composed of three stages for each process, as shown in Fig. 1, and a blanket roller covered with PDMS for ink transfer. A detailed explanation regarding the roll-offset printer or printing mechanism is available in a previous report [19]. As shown in Fig. 1 (a–b), the Ag nano-ink spin-coated onto an under-blanket at 5000 rpm was completely transferred to a PDMS roller at a speed of 5 mm/s with a force of 6 kgf. The Ag nano-ink covering the PDMS roller was patterned using a cliché at a speed of 1 mm/s with a force of 3 kgf, as shown in Fig. 1(c). Any patterned Ag nano-ink remaining on the PDMS roller was completely transferred to the glass or polymer substrate at a speed of 5 mm/s with a force 6 kgf, as shown in Fig. 1(d). The clichés were made of stainless steel, on which the mesh grids were patterned via laser etching. The transmittance of the mesh patterns was designed for 95% by changing the ratio of the line width (20–80 μm) to the pitch (800–3200 μm). The printed Ag nano-ink was sintered at 250 °C for 30 min in air.

Poly(3,4-ethylenedioxythiophene):poly(styrenesulfonate) (PEDOT:PSS, Agfa-Gevaert, Orgacon S305) was used in conjunction with the printed Ag mesh patterns to level the bottom electrode, which is remarkably transparent and a good hole conductor. The PEDOT:PSS was spin-coated on top of printed Ag mesh patterns at 800 rpm for 20 s and then cured under ambient conditions at 140 °C for 10 min.

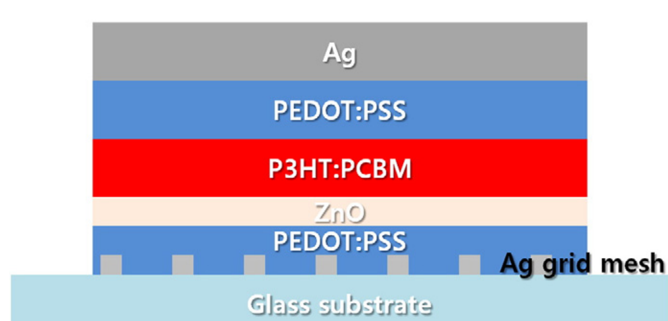

Fig. 2. A schematic illustration of the device architecture used in this study.